Electronic Supporting Information

A novel hydrophilic polymer-brush pattern for site-specific capture of blood cells from whole blood

Jianwen Hou,[ab] Qiang Shi,*[a] Wei Ye,[ab] Qunfu Fan,[c] Hengchong Shi,[a] Shing-Chung Wong,[d] Xiaodong Xu[c] and Jinghua Yin*[a]

[a] State Key Laboratory of Polymer Physics and Chemistry, Changchun Institute of Applied Chemistry, Chinese Academy of Sciences, Changchun 130022, P. R. China.

[b] University of Chinese Academy of Sciences, Beijing 100049, P. R. China.

[c] Polymer Materials Research Center, College of Materials Science and Chemical Engineering, Harbin Engineering University, Harbin 150001, P. R. China.

[d] Department of Mechanical Engineering, University of Akron, Akron, Ohio 44325-3903, USA.

*Corresponding author: shiqiang@ciac.ac.cn; yinjh@ciac.ac.cn

1. Experimental Section:

1.1 Materials.

SEBS copolymer with 29 wt% styrene (Kraton G 1652E, M_n=74800) was purchased from Shell Chemicals (USA). Benzophenone (BP) was supplied by Peking Ruichen Chemical (China). 2-Acrylamido-2-methylpropane sulfonic acid (AMPS) was purchased from Yuyuan Chemistry Company (Shandong, China). Acrylamide (AAm) (99.9%), Copper (II) bromide ($CuBr_2$, 99%) and 2, 2'-bipyridine (Bpy, >99%) were purchased from Alfa Aesar. Poly(ethylene glycol) methyl ether methacrylate (OEGMA) monomer (*Mn*~500), 2-Hydroxyethyl methacrylate (HEMA), 3-[Dimethyl-[2-(2-methylprop-2-enoyloxy) ethyl] azaniumyl] propane-1-sulfonate (SBMA), Copper (I) bromide (CuBr, 98%) were obtained from Sigma-Aldrich. Fibronectin (FN) was purchased from Beijing Solarbio Science & Technology Co., Ltd. (Beijing, China). Phytohemagglutinin (PHA) was obtained from Aladdin industrial corporation (Shanghai, China). FITC-fibronectin (FITC-FN) and rhodamine-phytohemagglutinin (RBITC-PHA) were purchased from Beijing biosynthesis biotechnology (China). Phosphate buffered saline (PBS, 0.1 mol L^{-1}, pH 7.4) and isotonic saline (NaCl solution, 0.154 mol L^{-1}, pH 7.4) were freshly prepared. Other chemicals were analytical grade and used without further purification. Milli-Q water (18.2 MΩcm) was used in all experiments.

1.2 Characterization.

ATR-FTIR Measurements.

The infrared spectra were measured in a Bruker FTIR spectrometer Vertex 70 equipped with an Attenuated Total Reflection (ATR) unit (ATR crystal 45°) at a resolution of 4 cm^{-1} for 32 scans.

XPS Measurements.

The surface composition was determined via X-ray photoelectron spectroscopy (XPS) by using VG Scientific ESCA MK II Thermo Avantage V 3.20 analyzer with Al/K (hν =1486.6 eV) anode mono-X-ray source. All the samples were completely vacuum dried before characterization. The take-off angle for photoelectron analyzer was fixed at 90°. All binding energy (BE) values were referenced to the C_{1s} hydrocarbon peak at 284.6 eV. The atomic concentrations of the elements were calculated by their corresponding peak areas.

POM.

The morphologies of the patterned surface were observed by polarized optical microscopy (Zeiss Axio Imager A2m, Carl Zeiss, Germany) equipped with a video CCD camera.

SEM.

Obtained substrates were observed with field emission scanning electron microscopy (FESEM) by using a XL 30 ESEM FEG (FEI Company) instrument equipped with an EDX spectroscopy attachment.

AFM.

The film morphologies were characterized by tapping-mode using a SPI 3800/SPA 300HV AFM (Seiko Instruments Inc., Japan). All measurements were carried out at room temperature in ambient air conditions.

CLSM.

Images were acquired by using a confocal laser scanning microscope (CLSM) (LSM700–Zeiss, Germany) equipped with an InGaN semiconductor laser (405 nm), an Ar laser (488 nm), and a He–Ne laser (555 nm). All samples were visualized using the same acquisition settings and analyzed using Zen 2011 software (Carl Zeiss).

Water Contact Angle Measurements.

Water contact angles were determined by the sessile drop method with a pure water droplet (ca. 3 μL) using a contact angle goniometer (DSA, KRUSS GMBH, Germany). The average value of five measurements made at different surface locations on the same sample was adopted as the contact angle.

1.3 Preparation of SEBS Films.

The SEBS film was prepared by dissolving 7 g of SEBS powder in 50 mL of dimethyl benzene. The polymer solution was then cast onto a glass substrate, and the solvent was removed by controlled evaporation at room temperature over a period of 48 h. And the thickness of the film was about 200 μm.

1.4 Preparation of Poly(AMPS)-Grafted SEBS.

For the surface-initiated photo-polymerization (SIPP) with AMPS, flat SEBS films were immersed in an ethanol solution of BP (1.5 wt %) for 30 min and then dried in vacuo under dark condition for 1 h at 25 °C. Monomer solution was prepared prior to the experiments by mixing AMPS monomer (3.2 g) in degassed DI water

(36.8 mL) and then argon was bubbled for 30 min to eliminate any oxygen. The BP-preadsorbed SEBS films were put on the slide glasses and coated with 8 wt % aqueous solution of AMPS, followed by covering with another quartz plate (0.8 mm thick). Then the sandwiched system was exposed to UV illumination (high-pressure mercury lamp, 400 W, main wavelength 380 nm) at a distance of 15 cm for 8 min at ambient temperature (22 °C). After SIPP, the samples were vigorously rinsed with deionized water and ethanol for 24 h to remove unreacted monomers and unreacted initiators. The samples were then dried in a vacuum oven for 24 h at room temperature. The so-obtained poly(AMPS)-grafted film was referred to as SEBS-*g*-PAMPS samples. Patterned SEBS-*g*-PAMPS sample was obtained using the copper grids as photomask when SIPP was conducted.

1.5 Fabrication of Patterned ATRP Initiator on SEBS-*g*-PAMPS Film.

The basic strategy for the fabrication of the patterned ATRP initiator using the aqueous-based method was adapted from our previous study.[1] Copper grids with different meshes (100-400) served as photomasks and SEBS-*g*-PAMPS samples incorporating copper grids were prepared in a cleanroom environment. Then they were exposed to UV/Ozone for 30 min in a cleaning chamber and were subsequently immersed in HBr/H_2SO_4 (5/1, v/v) mixture solution for 24 h at 60 °C. After that, these treated films were washed drastically with deionized water to remove physically adsorbed HBr and dried overnight under vacuum at 25 °C before use. The so-obtained films with immobilized patterned initiator were referred to as patterned brominated SEBS-*g*-PAMPS samples (SEBS-*g*-PAMPS-Br).

1.6 Formation of Patterned PAAm Brushes.

Briefly, CuBr (29.2 mg, 0.2 mmol), $CuBr_2$ (4.6 mg, 0.02 mmol) and patterned SEBS-*g*-PAMPS-Br samples were placed in a 100 mL round-bottom flask equipped with a glass stopper and then was subjected to laboratory vacuum followed by high pure argon gas in-flow for 30 min. A deoxygenated aqueous solution (water and methanol in a 1:1 volume ratio, 30 mL) with AAm (2 g, 28.14 mmol) and PMDETA (0.125 mL, 0.60 mmol) was introduced into the flask under argon protection. The resultant mixture was degassed through three freeze-pump-thaw cycles before the reaction started. The grafting process proceeded at 60 °C for a certain period of time. After the desired reaction time, substrates were removed from the polymerization solution, exhaustively rinsed with Milli-Q water to remove all traces of the polymerization solution, and subsequently dried under vacuum overnight at 25 °C. The as-prepared samples with grafted patterned PAAm brushes were referred to as patterned SEBS-*g*-PAMPS-*g*-PAAm samples.

1.7 Entrapment of Targeted Proteins on PAAm Brushes.

We have created a novel patterned PAAm brushes that can resist cells adhesion but promote proteins adsorption.[2] In this work, two cell adhesive proteins, FN and PHA, were selected as model proteins and a brief description of the adsorption procedure is given below.

FITC-FN and RBITC-PHA were dissolved in PBS at a concentration of 1 mg mL^{-1} and the patterned SEBS-*g*-PAMPS-*g*-PAAm substrates were incubated in the as-prepared protein solutions for 60 min at 37 °C in the dark. Following the incubation,

protein solutions were removed and the samples were gently washed twice with pre-warmed PBS (37 °C). Then the samples were dried under a stream of nitrogen and fluorescent images were observed with a CLSM (LSM700-Zeiss, Germany). As for the characterization of CLSM, the FITC and RBITC dyes were excited with an argon ion laser at 488 nm and 555 nm, respectively.

The adsorption of FN and PHA without fluorescence labeling on patterned surface was performed according to procedure described above. And the FN-adsorbed and PHA-adsorbed patterned SEBS-*g*-PAMPS-*g*-PAAm substrates were used to capture platelets and erythrocytes, respectively.

1.8 Blood Cells Capture.

Platelets Capture.

Fresh blood from healthy white rabbits was extracted via venipuncture through a 19-gauge Butterfly needle into a standard blood collection tube containing 3.8 wt% sodium citrate [9:1 (v/v) blood/anticoagulant] (Blood collection from animals was carried out in accordance with the guidelines issued by the Ethical Committee of the Chinese Academy of Sciences.). The first portion of blood drawn was discarded to avoid contamination by tissue thromboplastin caused by puncture with the needle. The citrated whole blood was immediately centrifuged (1000 rpm, 15 min, 25 °C) to obtain platelet rich plasma (PRP). After equilibration with PBS, the FN-adsorbed patterned SEBS-*g*-PAMPS-*g*-PAAm substrates were placed in contact with PRP and incubated for 60 min at 37 °C under static conditions. Then PRP was removed with an aspirator and the samples were gently rinsed three times with PBS to remove non-

adhered platelets. Subsequently, captured platelets were fixed using 2.5 vol% glutaraldehyde in PBS for 10 h at 4 °C. Finally, the samples were freeze-dried and the platelets captured on the patterned sample surfaces were observed using FESEM and CLSM, respectively.

Erythrocytes Capture.

To isolate and purify the erythrocytes, we used the method described by Brooks *et al*.[3] Briefly, the whole blood sample was centrifuged at 1000 rpm for 15 min to separate erythrocytes, white blood cells (WBCs), and PRP. Then the plasma and buffy coat layers (PRP and WBCs) were carefully removed and discarded. Erythrocytes concentrates were washed three times with isotonic saline (0.9% w/v of aqueous NaCl solution, pH 7.4). Afterward, the erythrocyte pellets were resuspended in normal saline to obtain an erythrocyte suspension at 20% (v/v) hematocrit. Subsequently, 80 μL of erythrocyte suspension was dropped on the surface of PHA-adsorbed patterned SEBS-*g*-PAMPS-*g*-PAAm substrates and incubated at 37 °C for 60 min under static conditions to provide enough time to capture erythrocytes. After the incubation, the samples were carefully rinsed twice with pre-warmed PBS, followed by immersing in 3 mL of 2.5 vol% glutaraldehyde in PBS for 10 h at 4 °C to fix the captured erythrocytes. Finally, the samples were freeze-dried and the morphologies of captured erythrocytes on the sample surfaces were visualized using FESEM and CLSM, respectively.

Cell Capture from Whole Blood.

The blood cell capture from whole blood on patterned surface was performed according to procedure described in normal erythrocytes capture. Whole blood was used to substitute concentrated erythrocytes for cell capture.

2. Supplemental Figures:

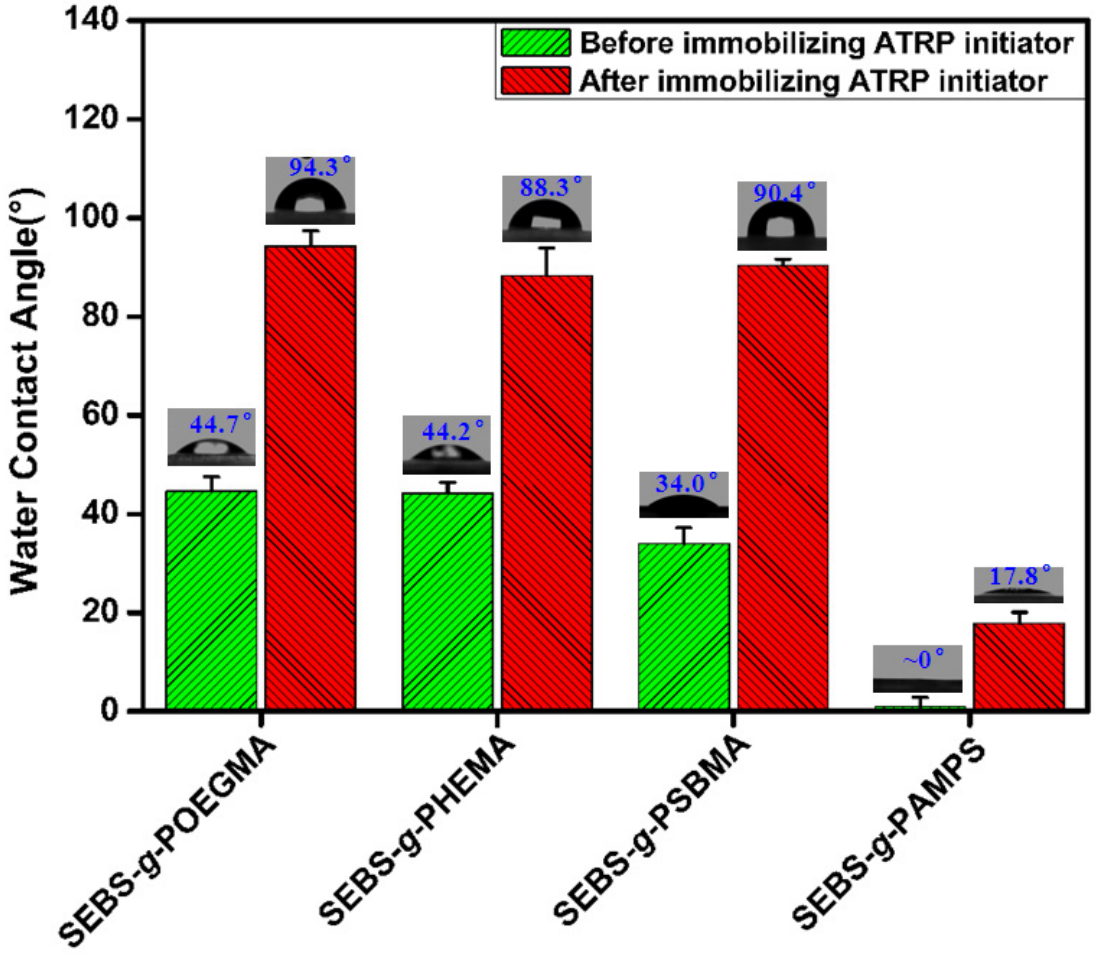

Figure S1. Water contact angle of functionalized SEBS surfaces grafted with different hydrophilic brushes before and after immobilizing ATRP initiator.

The initial polymer brushes must meet two requirements for successful creation of the platform for cell capture. (i) it should be hydrophilic in nature to offers better antifouling and cell resistance; (ii) it should be stable to maintain hydrophilic after generation of the ATRP initiators in the UV/Ozone-exposed areas with bromination reactions. Thus, selection of appropriate monomer to form initial polymer brushes is very important. Considering various types of hydrophilic monomers, such as poly (ethylene glycol) methacrylate (OEGMA),[4,5] 2-hydroxyethyl methacrylate

(HEMA),[6,7] sulfobetaine methacrylate (SBMA),[8,9] and 2-acrylamido-2-methylpropane sulfonic acid (AMPS),[10,11] are widely used as antifouling materials for resisting protein adsorption and cell attachment. We graft OEGMA, HEMA, SBMA and AMPS onto SEBS surface via SIPP, respectively. Then all the grafted samples are immersed in HBr/H_2SO_4 (5/1, v/v) mixed solution at 60 °C for 24 h. The wetting behavior of all the modified samples before and after bromination treatment is characterized by equilibrium contact-angle measurements (Figure S1). All the grafted samples exhibit relative hydrophilic property (less than 50°) and PAMPS-modified sample shows a superhydrophilic behavior (~0°). The water spreads completely and rapidly on the entire surface of SEBS-*g*-PAMPS (Video S1). After bromination treatment all the modified samples are hydrophobic (greater than 85°) except PAMPS-grafted sample, whose surface remain relative hydrophilic (17.8°). The above results indicate that only AMPS can keep its hydrophilic property after the ATRP initiator is immobilized onto the UV/Ozone exposed regions. Thus, PAMPS brushes are selected as the initial polymer brushes.

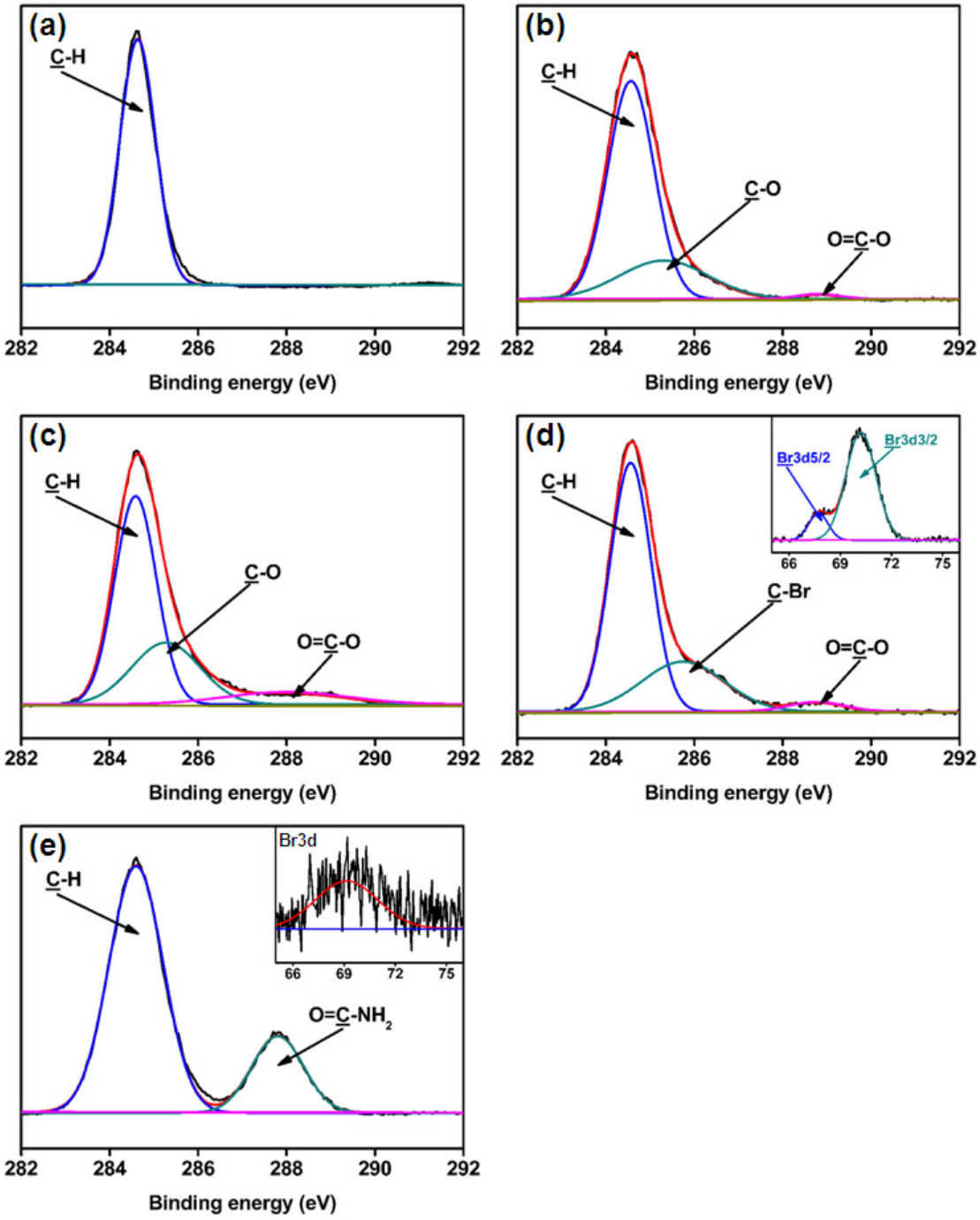

Figure S2. C_{1s} core-level spectra of (a) SEBS, (b) SEBS-*g*-PAMPS, (c) SEBS-*g*-PAMPS-OH, (d) SEBS-*g*-PAMPS-Br, (e) SEBS-*g*-PAMPS-*g*-PAAm samples. The insets of panel (d) and (e) are its corresponding Br_{3d} core-level spectra.

The high-resolution spectra corresponding to C_{1s} are shown in Figure S2 to distinguish different types of functional groups on the surfaces. In comparison with the single peak in C_{1s} spectrum of the virgin SEBS sample (Figure S2a), the C_{1s} spectrum of PAMPS-modified film shows three peaks at 284.6, 285.3 and 288.5 eV, attributing to the C-H, C-O, and O=C-O species, respectively. The results provide direct evidence of successful grafting of PAMPS brushes onto SEBS surface via SIPP (Figure S2b). Compared with SEBS-*g*-PAMPS film, the intensity of peaks at 285.3 eV (C–OH) and 288.5 eV (O–C=O) of UV/Ozone-treated SEBS-*g*-PAMPS sample (SEBS-*g*-PAMPS-OH) becomes much stronger (Figure S2c), indicating the UV/Ozone-treated sample are rich in hydroxyl and carboxylic acid groups on the surfaces. Successful anchoring of ATRP initiator onto the film surface is substantiated by the appearance of a new peak at 285.7 eV (C-Br) in the corresponding C_{1s} spectrum (Figure S2d). Due to the C-Br bond, the Br 3d spectrum of SEBS-*g*-PAMPS-Br film exhibits a broad peak at about 69 eV. The presence of PAAm brushes grown from the ATRP initiator is evidenced by the amide carbon O=C-NH_2 peak at 288.0 eV (Figure S2e). The presence of Br signal can be detected after ATRP process, showing that the grown PAAm chains retain the "controlled" character. And C-Br bonds connecting directly with activating substituents on the α-carbon, such as carbonyl groups, were confirmed to be the effective initiation sites.[1]

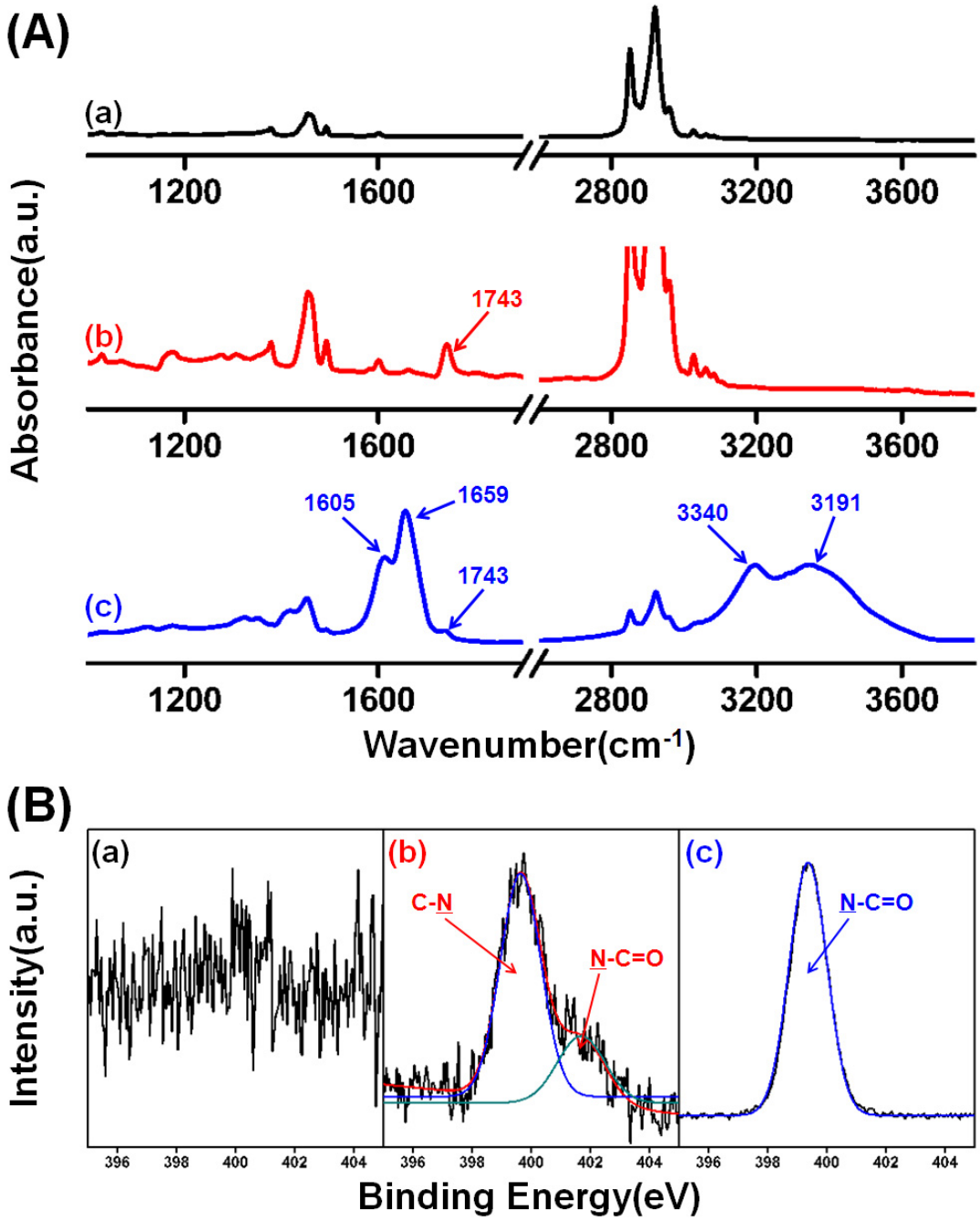

Figure S3. ATR-FTIR spectra and N_{1s} core-level spectra of (a) SEBS, (b) SEBS-*g*-PAMPS, (c) SEBS-*g*-PAMPS-*g*-PAAm samples.

The formation of two-component polymer brushes on the model surface is confirmed by ATR-FTIR (Figure S3A) and XPS spectra (Figure S3B). Compared with the FTIR spectrum of the virgin SEBS, new peaks at 1743 cm^{-1} (C=O stretching vibration of PAMPS) and 1659 cm^{-1} (C=O stretching vibration of PAAm) appear after grafting the initial PAMPS brushes and the second PAAm brushes, respectively. Similarly, there is no nitrogen signal on virgin SEBS surface. Two peaks at binding energies of 399.7 (C-N groups) and 401.8 eV (N-C=O groups) in the N_{1s} spectrum of SEBS-g-PAMPS are observed. But only a binding energy of 399.3 eV (N-C=O groups) appears after formation of PAAm brushes. The changes are due to the etching of PAMPS brushes by UV/Ozone radiation and generation of PAAm brushes.

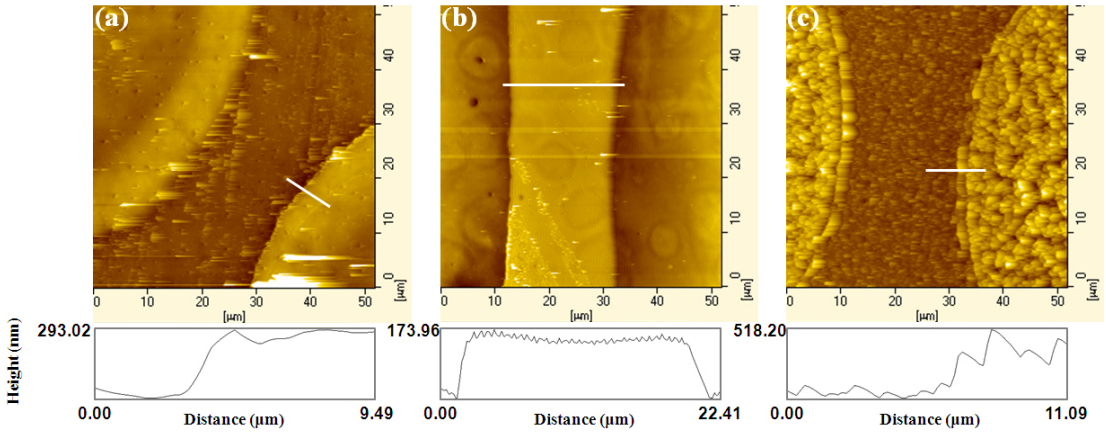

Figure S4. AFM images (50×50 μm^2) of the micropatterned SEBS surfaces and their corresponding height profiles along the line shown in the images. (a) SEBS-*g*-PAMPS surface, (b) SEBS-*g*-PAMPS-Br surface, (c) SEBS-*g*-PAMPS-*g*-PAAm surface.

Atomic force microscopy (AFM) has become a powerful tool for measuring the thickness of polymer brushes in recent years.[12] The model surfaces with the patterned polymer brushes made it possible for AFM to measure the brush thickness accurately. Figure S4 presents the AFM images and their corresponding thickness profiles of the micropatterned SEBS-*g*-PAMPS, SEBS-*g*-PAMPS-Br and SEBS-*g*-PAMPS-*g*-PAAm surfaces, respectively. As for the patterned SEBS-*g*-PAMPS sample, PAMPS brushes selectively grow on the UV/Ozone-irradiated areas. The thickness of PAMPS brushes is about 293 nm based on the thickness profile. In order to measure thickness of PAAm brushes, it is necessary to determine the thickness of SEBS-*g*-PAMPS-Br layer before SI-ATRP proceeds. Figure S4b shows an AFM image of patterned SEBS-*g*-PAMPS-Br sample, the relative height of the UV/Ozone-unexposed domains appears to be approximately 174 nm higher than that of UV/Ozone-exposed domains. This phenomenon is mainly caused by the etching process of UV/Ozone treatment.

UV/Ozone treatment leads to the decomposition of PAMPS brushes in the UV/Ozone-exposed regions.[13] After performing subsequent SI-ATRP of AAm, the overall height, as well as the height-profile, change significantly. The polymer brushes grow from the patterned initiators, resulting in regularly distributed microstructures. The relative height of the UV/Ozone-unexposed domains appears to be approximately 518 nm lower than that of UV/Ozone-exposed domains. So the thickness of the PAAm brushes is about 692 (518+174=692) nm.

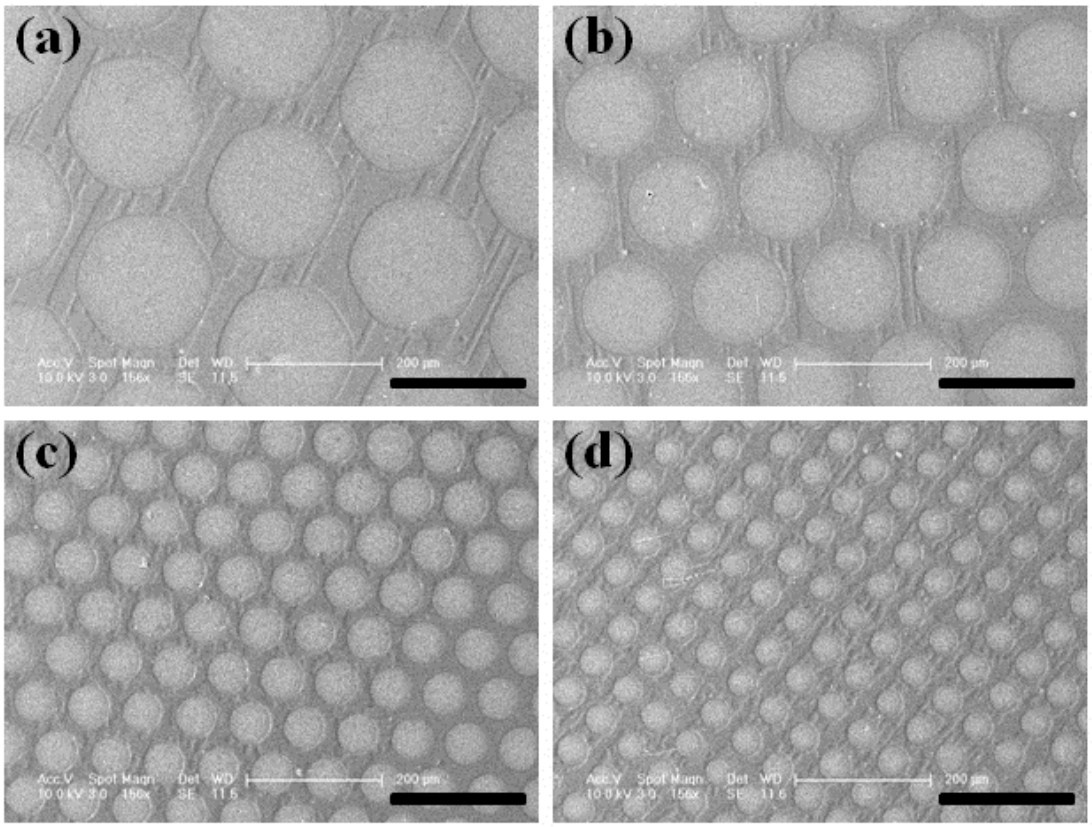

Figure S5. SEM images of two-component PAMPS/PAAm brush patterns with different sizes. Scale bar is 200 μm.

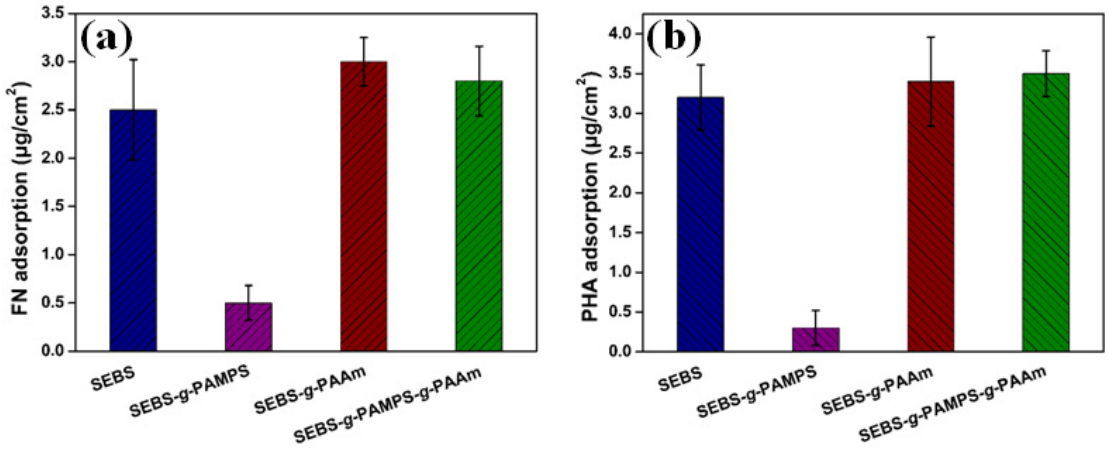

Figure S6. Total amount of adsorbed FN (a) and PHA (b) on different model surfaces.

A quantitative assessment of protein entrapment on different model surfaces is performed (Figure S6). Figure S6a and 6b show the total amount of entrapped FN and PHA on the surface of SEBS, SEBS-*g*-PAMPS, SEBS-*g*-PAAm and SEBS-*g*-PAMPS-*g*-PAAm, respectively. Compared with virgin SEBS, there are about 80% and 91% reductions of entrapped FN and PHA on SEBS-*g*-PAMPS surface, respectively. However, the amount of entrapped FN and PHA on the SEBS-*g*-PAAm surface is a little higher than that adsorbed on virgin SEBS surface, confirming the PAAm brushes obtained here have high ability to entrap targeted proteins. There are no obvious differences in protein entrapment between SEBS-*g*-PAAm and SEBS-*g*-PAMPS-*g*-PAAm, indicating that the underlying residual PAMPS brushes have slight effect on the entrapment capacity of PAAm brushes.

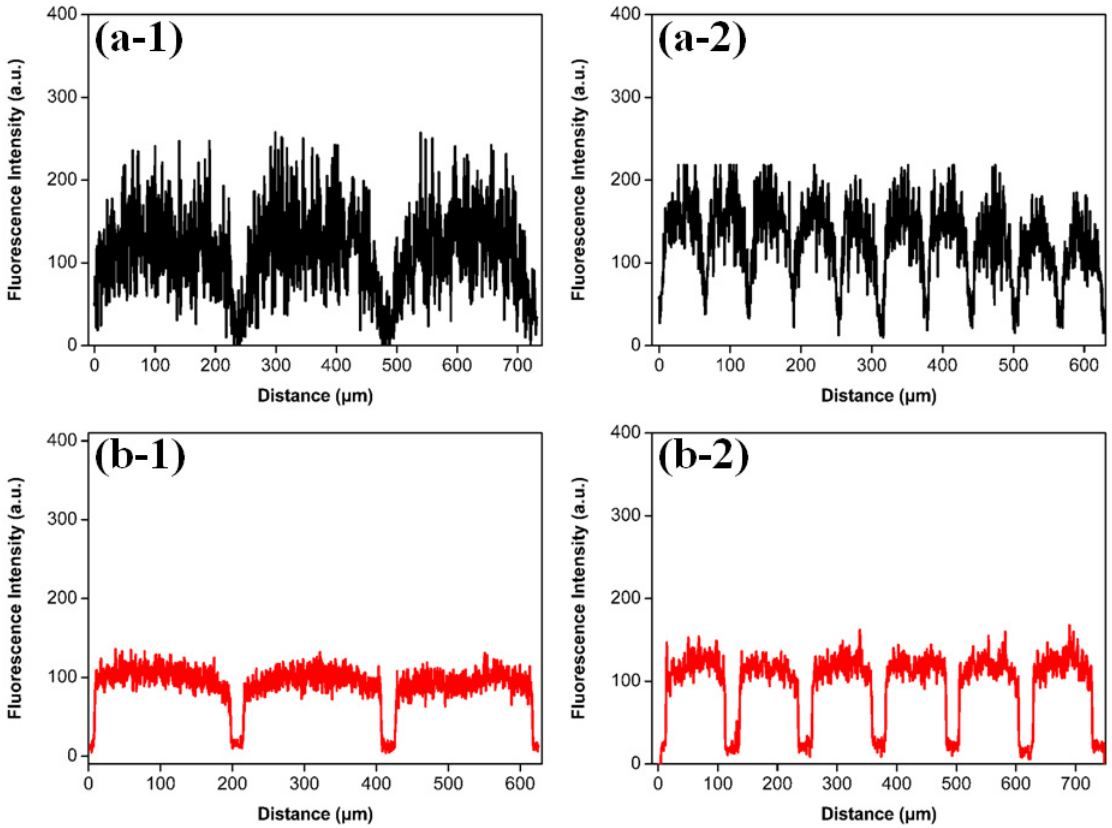

Figure S7. Fluorescence intensity profile of patterned surface after entrapment of FITC-FN (a1, a2) and RBITC-PHA (b1, b2).

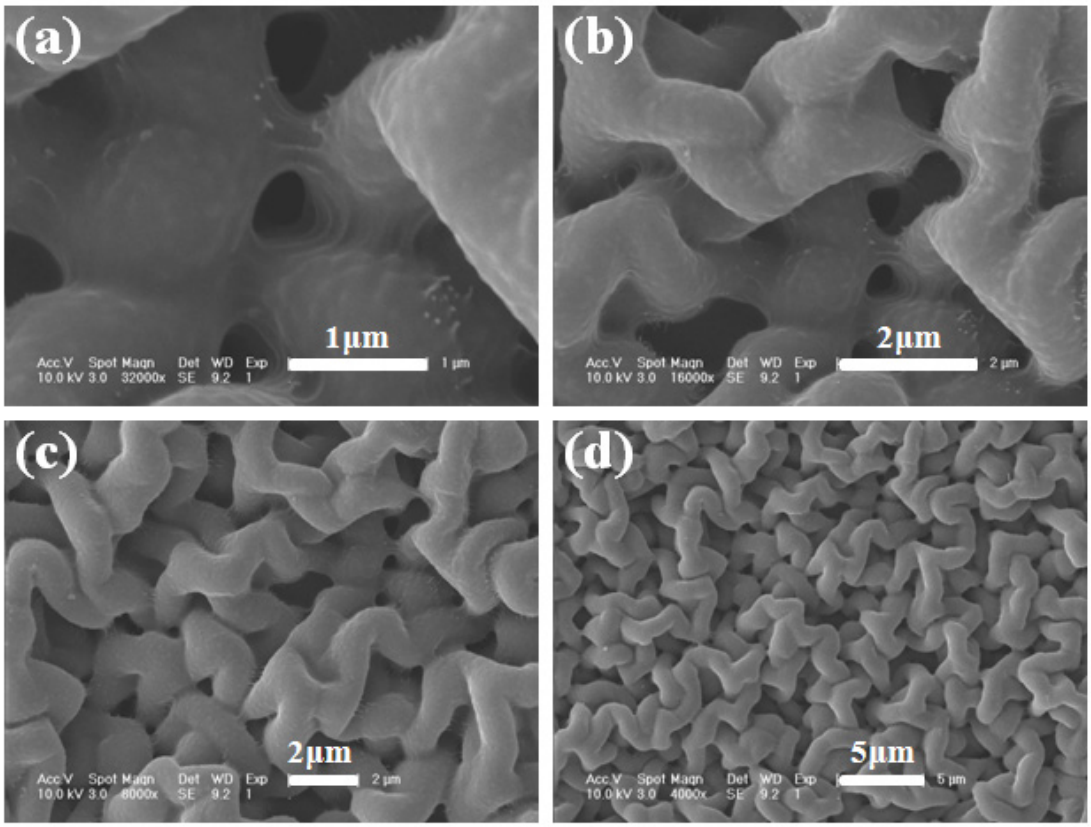

Figure S8. Different-magnification SEM images of the as-grown PAAm brushes from the substrate surface, showing the surface is fully populated with a hierarchically microstructure and irregular hydrogel-like networks.

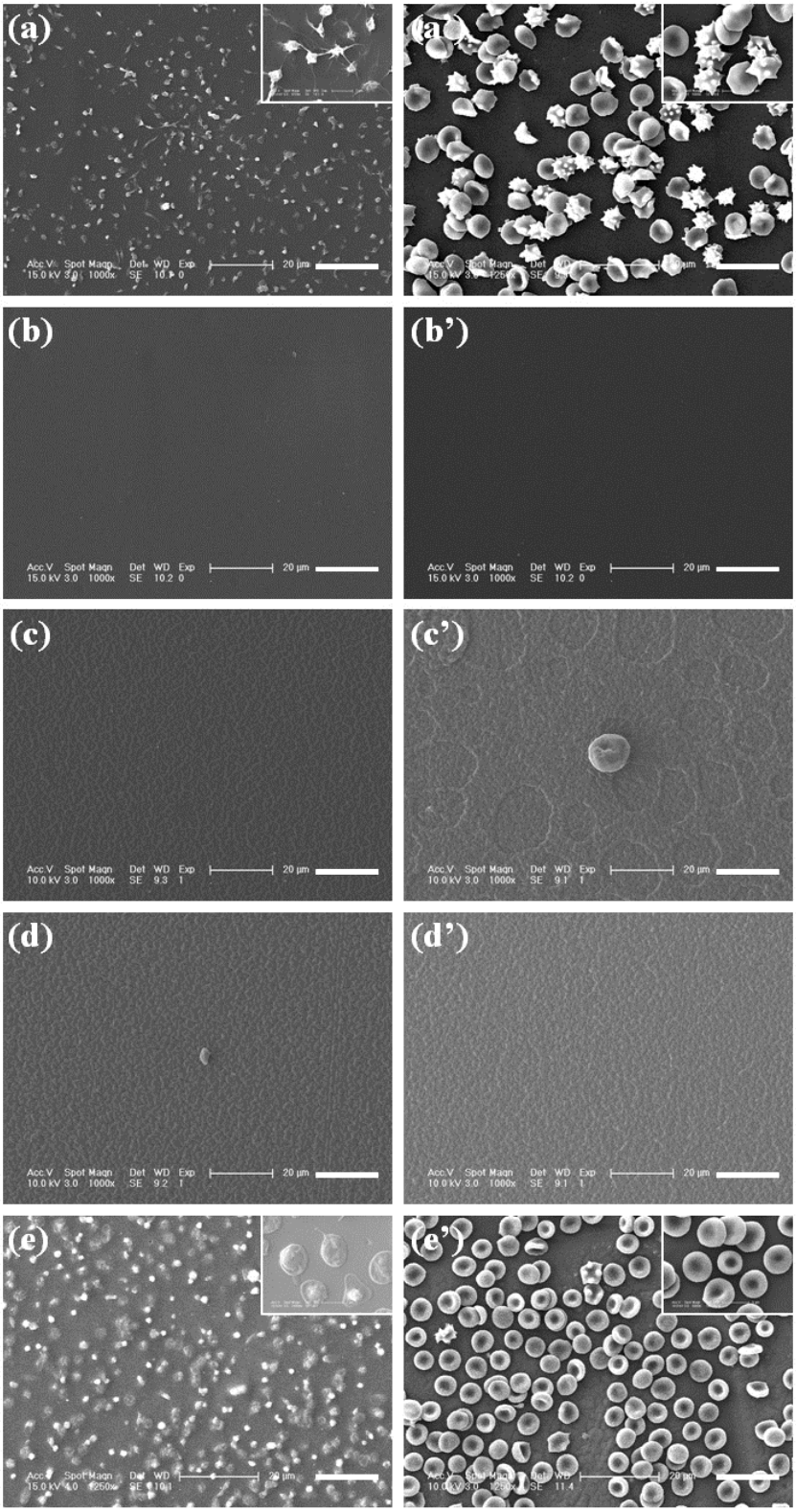

Figure S9. SEM images of adhered platelets (a-e) and erythrocytes (a'-e') on the surface of (a, a') virgin SEBS, (b, b') SEBS-*g*-PAMPS, (c, c') SEBS-*g*-PAAm, (d, d') SEBS-*g*-PAMPS-*g*-PAAm, and (e, e') SEBS-*g*-PAMPS-*g*-PAAm with FN and PHA, respectively. Scale bar is 20 μm.

3. Supplemental Tables:

Table S1. Chemical Composition and Static Water Contact Angle of the Functionalized SEBS Surfaces.

Sample	Compositions (at.%)					WCA (±3°)
	C(%)	O(%)	N(%)	S(%)	Br(%)	
SEBS	96.32	3.68	--	--	--	106
SEBS-*g*-PAMPS	78.40	15.14	3.54	2.92	--	~0
SEBS-*g*-PAMPS-Br	92.38	2.46	1.74	1.26	2.16	84
SEBS-*g*-PAMPS-*g*-PAAm	69.48	16.72	13.67	--	0.13	27

4. References:

1. J. Hou, Q. Shi, P. Stagnaro, W. Ye, J. Jin, L. Conzatti and J. Yin, *Colloids Surf., B*, 2013, **111**, 333-341.
2. J. Hou, Q. Shi, W. Ye, P. Stagnaro and J. Yin, *Chem. Commun.,* 2014, **50**, 14975-14978.
3. X. Yu, Y. Zou, S. Horte, J. Janzen, J. N. Kizhakkedathu and D. E. Brooks, *Biomacromolecules*, 2013, **14**, 2611-2621.
4. J. A. Castillo, D. E. Borchmann, A. Y. Cheng, Y. Wang, C. Hu, A. J. García and M. Weck, *Macromolecules*, 2011, **45**, 62-69.
5. Z. Lin, Y. Ma, C. Zhao, R. Chen, X. Zhu, L. Zhang, X. Yan and W. Yang, *Lab Chip*, 2014, **14**, 2505-2514.
6. Y. Zhang, N. Islam, R. G. Carbonell and O. J. Rojas, *Anal. Chem.*, 2012, **85**, 1106-1113.
7. M. Tao, F. Liu and L. Xue, *J. Mater. Chem.*, 2012, **22**, 9131-9137.
8. W. J. Yang, K.-G. Neoh, E.-T. Kang, S. L.-M. Teo and D. Rittschof, *Polym. Chem.*, 2013, **4**, 3105-3115.
9. S.-H. Chen, Y. Chang, K.-R. Lee, T.-C. Wei, A. Higuchi, F.-M. Ho, C.-C. Tsou, H.-T. Ho and J.-Y. Lai, *Langmuir*, 2012, **28**, 17733-17742.
10. H. Yin, T. Akasaki, T. L. Sun, T. Nakajima, T. Kurokawa, T. Nonoyama, T. Taira, Y. Saruwatari and J. P. Gong, *J. Mater. Chem. B*, 2013, **1**, 3685-3693.
11. L. Song, J. Zhao, H. Yang, J. Jin, X. Li, P. Stagnaro and J. Yin, *Appl. Surf. Sci.*, 2011, **258**, 425-430.

12. X. Sui, S. Zapotoczny, E. M. Benetti, P. Schön and G. J. Vancso, *J. Mater. Chem.*, 2010, **20**, 4981-4993.

13. A. M. Urbas, M. Maldovan, P. DeRege and E. L. Thomas, *Adv. Mater.,* 2002, **14**, 1850-1853.